Applied Surface Science 258 (2012) 9792–9799

Contents lists available at SciVerse ScienceDirect

Applied Surface Science

journal homepage: www.elsevier.com/locate/apsusc

Facile morphological control of single-crystalline silicon nanowires

Shao-long Wu, Ting Zhang, Rui-ting Zheng, Guo-an Cheng*

Key Laboratory of Beam Technology and Material Modification of Ministry of Education, College of Nuclear Science and Technology, Beijing Normal University, Beijing 100875, PR China

ARTICLE INFO

Article history:
Received 13 December 2011
Received in revised form 6 June 2012
Accepted 10 June 2012
Available online 18 June 2012

Keywords:
Morphological control
Vertically-aligned nanowires
Slanting-aligned nanowires
Zigzag silicon nanowires
Porosity
Rough surface

ABSTRACT

To realize wider potentials of silicon nanowires (SiNWs), the morphological controllability is desirable. In this paper, we synthesized well vertically- and slantingly-aligned SiNWs with ultra-high aspect ratio in metal-assisted chemical etching method, and wafer-scale zigzag SiNWs with three types of turning angle were also obtained. The formation of the curved SiNWs is a result of the alternation of moving direction of Ag nanoparticles between the preferred ⟨1 0 0⟩ and other directions in Si substrates. The as-prepared SiNWs are single-crystalline and their orientations are mostly along the ⟨1 0 0⟩ or ⟨1 1 1⟩ directions. The surface of the resulting SiNWs can be controlled to be smooth or rough, with or without mesopores, by adjusting the etching conditions and using various Si substrates with different crystal orientations and doping levels. Moreover, the effects of the etching conditions (etching time, oxidant concentration, deposition time of Ag nanoparticles and etching temperature) and substrate properties (crystal orientation and doping level) on the as-prepared SiNWs have been discussed.

© 2012 Elsevier B.V. All rights reserved.

1. Introduction

One dimensional (1D) silicon nanowires (SiNWs) have been intensively investigated for their novel optical, electronic and chemical properties [1–3]. Various functional nanoscale devices based on SiNWs have been reported, such as field-effect transistors [4], solar cells [5], photodetectors [6], solid-state thermoelectric devices [7] and so on. The morphology of SiNWs, as much as the intrinsic properties, plays a decisive role in their applications, especially in the nanoscale devices of a single nanowire. Thus, it is very necessary to control morphology of SiNWs for further improving their novel properties and opening expansive applications.

Various methods of fabricating SiNWs have been reported, like vapor–liquid–solid (VLS) growth [8], solid–liquid–solid (SLS) growth [9], oxide-assisted growth [10], and vapor–solid–solid (VSS) growth [11]. Via the dry [12] or wet [13] etching methods with a patterned mask, the SiNWs with controlled size and density can be obtained. Nevertheless, the control of the orientation and surface topography is relatively complicated and high-cost in these methods. Here, we used the metal-assisted chemical etching method, which has attracted wide attention because of its low cost and capability to prepare well-aligned arrays with controlled optoelectronic properties [14,15]. The wafer-scale vertically-, slantingly-aligned and zigzag SiNWs were fabricated by adjusting the etching conditions and using various Si substrates with different orientations and doping levels, and the surface topography of the resulting SiNWs can be facilely controlled.

2. Experimental

Wafer-scale SiNWs were prepared by metal-assisted chemical etching of n-type Si(1 0 0, 1–10 Ω cm), p-type Si(1 0 0, 0.005–0.025 Ω cm), p-type Si(1 1 0, 75–150 Ω cm), and n-type Si(1 1 1, 0.01–0.02 Ω cm) wafers, similarly to our previous report [16]. Firstly, Si chips were ultrasonically cleaned in acetone, ethanol and de-ionized water for 15 min, respectively. And then the Si chips were boiled in the 3:1 mixture of 97% H_2SO_4 and 30% H_2O_2 for 30 min. Secondly, the cleaned Si chips were dipped into the $AgNO_3$/HF solution for electroless deposition of Ag nanoparticles (AgNPs) at room temperature (∼20 °C). Subsequently the AgNP-coated Si chips were immersed into the H_2O_2/HF solution for chemical etching. The oxidant (H_2O_2) concentration, deposition time of AgNPs, etching time and etching temperature were adjusted for obtaining various morphologies. Finally, the as-etched Si chips were soaked in 50% HNO_3 to remove the residual AgNPs, cleaned with de-ionized water and dried naturally in air.

The morphological and structural characterizations of SiNWs were examined by a field emission scanning electron microscope (FE-SEM, S-4800, Hitachi), a transmission electron microscope (TEM, Tecnai-T20, Philips), and a high resolution transmission electron microscope (HR-TEM, JEM-2010, JEOL). For the SEM observation, the wafer-scale SiNWs were cut into small pieces for the top and cross-sectional views. Furthermore, the as-prepared SiNWs were scratched by a scalpel into ethanol for ultrasonic dispersion.

* Corresponding author. Tel.: +86 010 62205403; fax: +86 010 62205403.
E-mail address: gacheng@bnu.edu.cn (G.-a. Cheng).

0169-4332/$ – see front matter © 2012 Elsevier B.V. All rights reserved.
http://dx.doi.org/10.1016/j.apsusc.2012.06.031

Afterwards, a drop of the solution was dipped on a piece of polished cleaned Si for SEM observation, and on a Cu grid covered with carbon support film for TEM observation, respectively.

3. Results and discussion

3.1. Wafer-scale vertically- and slantingly-aligned SiNWs with ultra-high aspect ratio

Well vertically- and slantingly-aligned SiNWs with ultra-high aspect-ratio were fabricated by chemical etching of various Si substrates with various etching conditions. The forming process of SiNWs can be described as follow: AgNPs are firstly deposited via Ag^+ reduction in the $AgNO_3$/HF solution, and then induce the Si at Ag/Si interfaces to be oxidized by H_2O_2 and then dissolved by HF, leaving tunnels into Si wafers. Due to the high density of AgNPs, neighboring tunnels might merge together leaving SiNWs in between [14]. This etching process indicates that the morphology of SiNWs may be controlled by controlling the distribution and sizes of AgNPs and their migration directions in Si substrates. Fig. 1a shows the vertically-aligned SiNWs with a length of ∼108 μm, the inset indicates the diameters of SiNWs ranging from 20 nm to 300 nm. This sample was prepared by dipping the as-cleaned Si(1 0 0, 1–10 Ω cm) chip in the aqueous solution of 0.01 M $AgNO_3$ and 4.0 M HF for 1 min, following immersing in the aqueous solution of 0.2 M H_2O_2 and 4.8 M HF for 3 h at room temperature. The ultra-high-aspect-ratio upstanding SiNWs implies that the Si etching is anisotropic and the movement of AgNPs is along the ⟨1 0 0⟩ directions. Based on the above discussions, we used Si(1 1 0) wafers to grow SiNWs for probing into the moving direction of AgNPs in the other substrates with different crystal orientations. Fig. 1b shows the typical SEM images of slantingly-aligned SiNWs, which were obtained from Si(1 1 0, 75–150 Ω cm) wafers via electroless deposition of AgNPs in the aqueous solution of 0.01 M $AgNO_3$ and 4.0 M HF for 150 s, following chemical etching in the aqueous solution of 0.4 M H_2O_2 and 4.8 M HF for 30 min at 50 °C. These experiments demonstrated that the moving direction of AgNPs in Si(1 1 0) wafers is along the ⟨1 0 0⟩ directions, forming the slantingly-aligned SiNWs. It may be interpreted by the lattice configuration of Si surfaces: the (1 0 0) plane possesses two covalent bonds symmetrically directed into the reactive solution and the smallest energy barrier for etching, leading to the slanted SiNWs orientated along the ⟨1 0 0⟩ directions [17,18]. These results demonstrate that the vertically- and slantingly-aligned SiNWs can be synthesized by optimizing etching conditions and using different Si substrates, and the unique morphology has promising applications like bionics, energy harvest and environmental governance [19].

3.2. Zigzag SiNWs prepared by chemical etching of Si(1 1 1) wafers.

The morphology of chemical etched Si(1 1 1) wafers appears to be more complicate than that of Si(1 0 0) and Si(1 1 0) wafers. There are two distinct directions of AgNP movement in the Si(1 1 1) substrates, which is also observed in other reports [18,20]. Our experiments imply that the moving direction of AgNPs is mainly determined by the AgNP size and the etching temperature. Fig. 2 shows the morphology of the as-synthesized SiNWs on Si(1 1 1) wafers etched in the aqueous solution of 0.4 M H_2O_2 and 4.8 M HF for 30 min at room temperature, with various deposition time of AgNPs in the aqueous solution of 0.005 M $AgNO_3$ and 4.8 M HF. It can be seen that: (1) the etching tracks are vertical to the Si substrates when the deposition time of AgNPs is short, forming high-density upstanding 1D nanostructures (as shown in Fig. 2a and d); (2) uniform slantingly-aligned SiNWs are synthesized when the deposition time of AgNPs is long enough (as shown in Fig. 2g and h); (3) there are direction transformations of AgNP movement when the deposition time is around 120 s. We infer that small-size AgNPs induce Si etching along the ⟨1 1 1⟩ directions, and large-size AgNPs induce Si etching along the ⟨1 0 0⟩ directions. The various directions of AgNP tracks can be understood by that the sizes of AgNPs are slowly reduced when they catalytically induce Si etching. The AgNPs are firstly oxidized by H_2O_2, and then capture electrons from the Si at Ag/Si interfaces, but the Ag^+ ions are not 100% reduced at the interfaces [14]. The small-size AgNPs may perform stronger catalytic activity, resulting in that the direction of AgNP movement in Si substrates transfers from the ⟨1 0 0⟩ to ⟨1 1 1⟩ directions, where the potential barrier of Si etching is larger than that along the ⟨1 0 0⟩ directions.

Fig. 3 shows the well-aligned SiNWs produced by depositing AgNPs in the aqueous solution of 0.01 M $AgNO_3$ and 4.8 M HF for 150 s and following etching in the aqueous solution of 0.4 M H_2O_2 and 4.8 M HF for 30 min at various temperatures. The SiNWs synthesized at 20 °C are slanted to the substrates, but the SiNWs formed at 50 °C are vertically-aligned. The average sizes of AgNPs in this case are relatively large for 150 s of AgNP deposition, the direction of AgNP movement should be along the ⟨1 0 0⟩ directions according to the above discussions. However, the vertically-aligned SiNWs were obtained when the etching temperature was around 50 °C, namely the direction of AgNP movement is changed to be along the ⟨1 1 1⟩ directions. The fact of AgNP moving along the ⟨1 1 1⟩ directions, where the interatomic bonds are stronger than that in the ⟨1 0 0⟩ directions, implies that the catalytic activity of AgNPs may be improved when the etching temperature is enhanced.

To further investigate the AgNP tracks in Si(1 1 1) substrates, we carried out additional numbers of etching experiments with

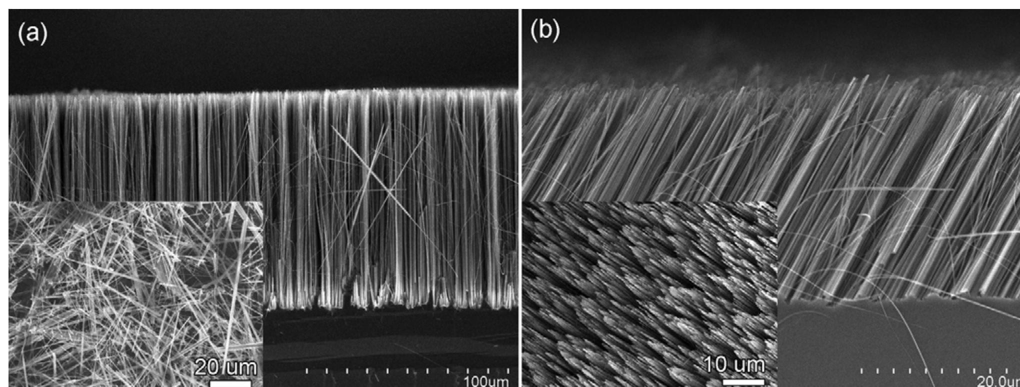

Fig. 1. (a) Cross-sectional SEM image of vertically-aligned SiNWs. Inset is the top view of SiNWs scraped and dispersed on a polished Si substrate. (b) Cross-sectional SEM image of slantingly-aligned SiNWs. Inset is the corresponding top view.

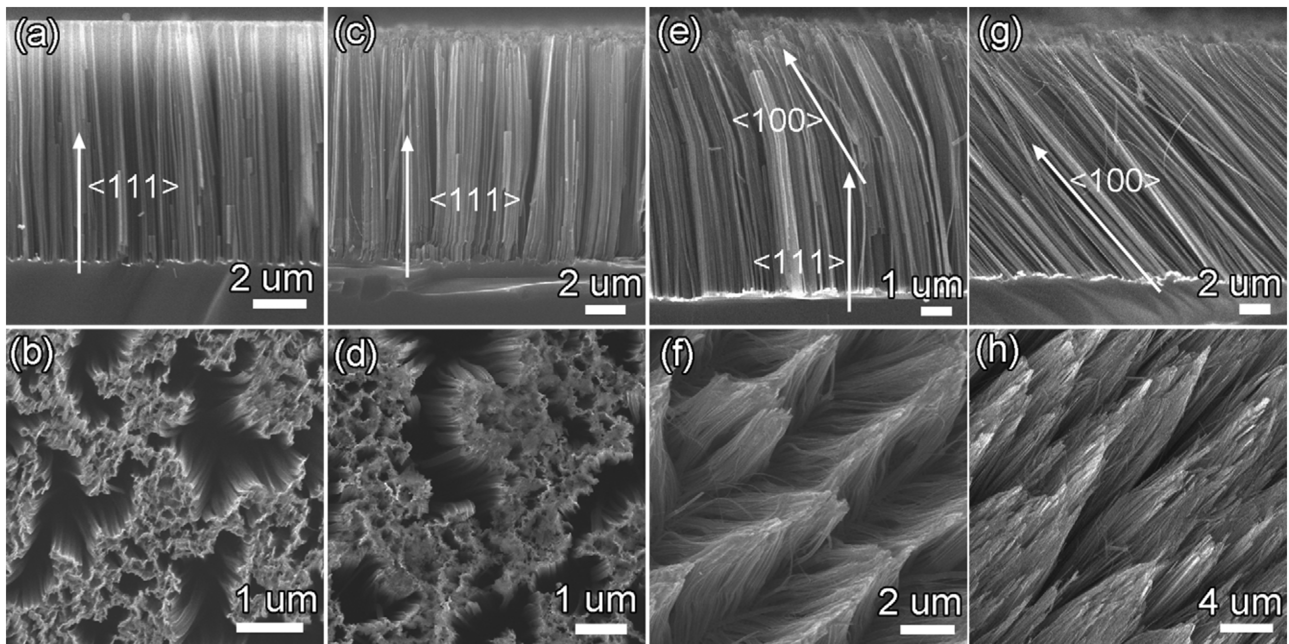

Fig. 2. Typical SEM images of the as-synthesized SiNWs from Si(1 1 1) wafers with various deposition time of AgNPs. Cross-sectional (a) and top views (b) of the SiNWs with deposition time of 30 s. Cross-sectional (c) and top views (d) of the SiNWs with deposition time of 60 s. Cross-sectional (e) and top views (f) of the SiNWs with deposition time of 120 s. Cross-sectional (g) and top views (h) of the SiNWs with deposition time of 180 s.

various etching conditions. Three types of curved SiNWs were observed. Fig. 4a shows cross-sectional SEM images of the SiNWs with 125° turning angle, which corresponds to the included angle between the ⟨1 0 0⟩ and ⟨1 1 1⟩ directions. Fig. 4b implies that the moving direction of AgNPs may be changed from one ⟨1 0 0⟩ to another ⟨1 0 0⟩ direction in the process of Si etching, leaving curved SiNWs with 90° turning angle. Fig. 4c shows there are uniform zigzag nanostructures with turning angle of 150° in the bottom segment of SiNWs. It is also observed in Chen's report [20], which proposed that the zigzag structures were synthesized from the AgNP-moving-direction alternating between the ⟨1 1 1⟩ and ⟨1 1 3⟩ directions periodically. Much longer zigzag SiNWs were obtained

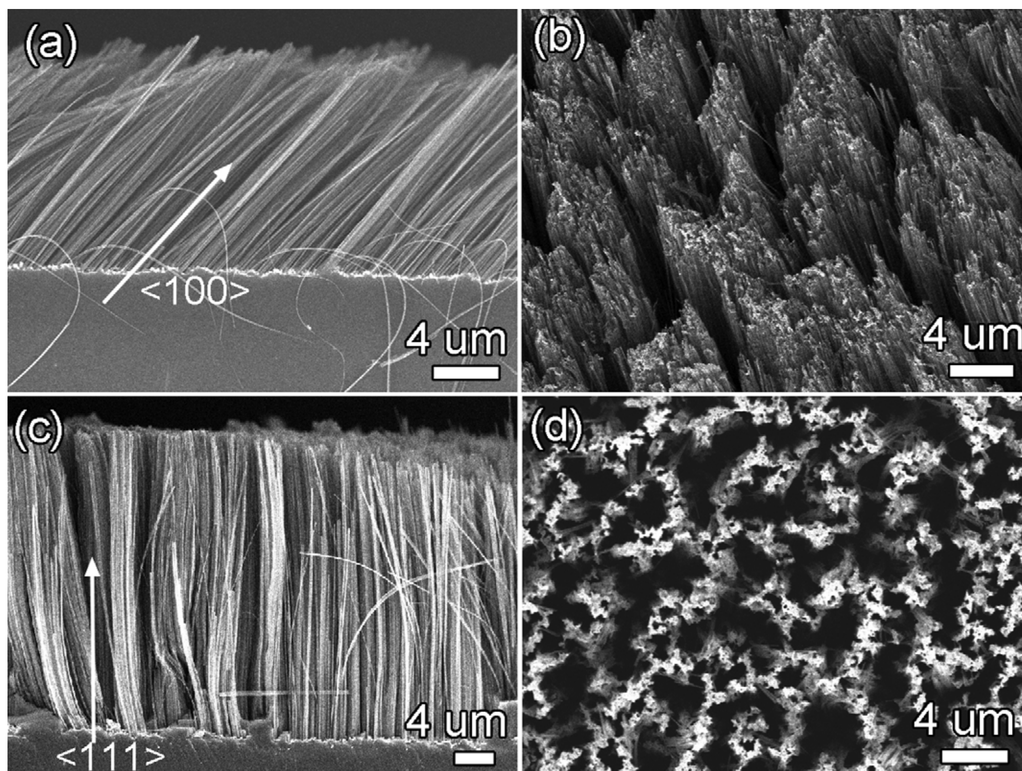

Fig. 3. Various morphological SEM images of the as-synthesized SiNWs produced from Si(1 1 1) wafers at two different etching temperatures. Cross-sectional (a) and top (b) views of the SiNWs etched at ~20 °C. Cross-sectional (c) and top (d) views of the SiNWs etched at ~50 °C.

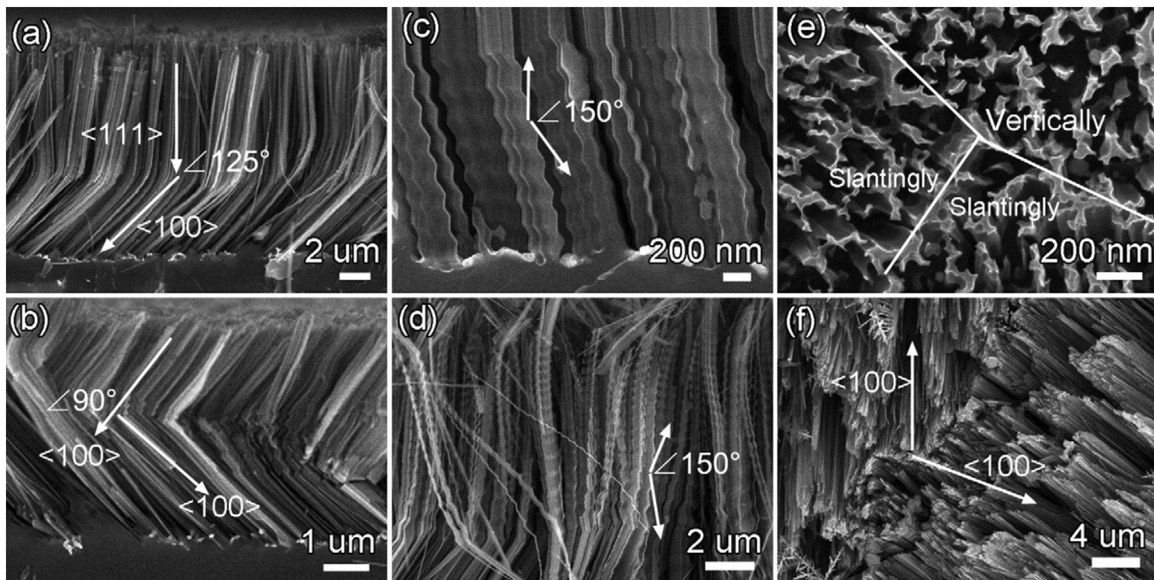

Fig. 4. Various AgNP moving tracks induce zigzag SiNWs. (a) AgNP tracks transfer from the ⟨1 1 1⟩ to ⟨1 0 0⟩ directions, leaving 125° turning angle. (b) AgNP tracks alter between two different ⟨1 0 0⟩ directions, leaving 90° turning angle. Zigzag SiNW arrays with 150° turning angle located at the bottom (c) middle segment (d) of SiNWs. (e) Top-view SEM image of different tunnels along different directions produced by AgNP movements in Si substrates for one min. (f) Top-view SEM image of the slantingly-aligned SiNWs along two different ⟨1 0 0⟩ directions.

by increasing H_2O_2 concentration and etching time, as shown in Fig. 4d. The zigzag segments are located in the middle of SiNWs, and the lengths of the waved nanostructures are up to 10 μm. Fig. 4e shows top-view SEM image of the AgNP tunnels in Si(1 1 1) substrates for 1-min etching. Note that the initial moving directions of AgNPs are inconsonant, there are tunnels either slanting or vertical to the substrates. It is not agree with Chen's viewpoint [20], which inferred that the AgNPs would first start moving perpendicular to the wafers along the ⟨1 1 1⟩ directions and then either may keep moving along the ⟨1 1 1⟩ or other directions such as ⟨1 0 0⟩ or ⟨1 1 3⟩. Fig. 4f is the top-view SEM image of SiNWs with different slanted orientations, suggesting that the AgNP movements are preferred to the ⟨1 0 0⟩ directions, and the various ⟨1 0 0⟩ directions of AgNP tracks may emerge at the beginning of chemical etching.

Fig. 5 shows the TEM images of single SiNW from typically vertically- and slantingly-aligned arrays. It can be observed that the surfaces of the two SiNWs are very rough and there are numbers of disordered mesopores. HRTEM analysis demonstrated the orientations of the two SiNWs from vertically- and slantingly-aligned arrays are along the ⟨1 1 1⟩ and ⟨1 0 0⟩ directions, respectively, which is in accord with the SEM analysis. The orientation of Si etching is along one of the three different ⟨1 0 0⟩ directions by random, and the different AgNPs at different positions might collectively move along the same direction, leaving SiNW arrays on the substrates. The AgNP-movement alternating between the ⟨1 0 0⟩ and ⟨1 1 1⟩ directions would result in the curved SiNWs with a 125° turning angle. By such analogy, the SiNWs with a 90° turning angle are synthesized when the AgNP tracks alter between two different ⟨1 0 0⟩ directions. These results demonstrate that the metal-assisted chemical etching is a facile and effective approach for fabrication of wafer-scale zigzag single-crystalline SiNWs.

3.3. Various surface topographies of SiNWs

We have demonstrated that the shapes of SiNWs are controllable, but the control of surface topography of SiNWs is not involved and it is unclear that how these mesoporous surfaces of SiNWs were produced from Si(1 1 1, 0.01–0.02 Ω cm) wafers (as shown in Fig. 5). In the next part of this paper, we will show various surface topographies of SiNWs and figure it out that how these surface mesopores are formed. Since the SiNWs are synthesized via the Si etching at Ag/Si interfaces, the doping level of Si substrates, H_2O_2 concentration, etching time and etching temperature should take an important part in the formation of various surface topographies. Fig. 6 shows the SEM and TEM images of the SiNWs produced from Si(1 0 0, 1–10 Ω cm) wafers with various conditions. It can be observed that as the etching time increases from 20 min to 60 min, the lengths of SiNWs increase from ∼7.5 μm to ∼23 μm, but the density of SiNWs is significantly reduced. What is more, the surface topographies of the SiNWs synthesized with markedly different etching time are obviously different. The surfaces of short-time-etching SiNWs are smooth, but the surfaces of long-time-etching SiNWs are rough. The increasing roughness may arose from the secondary AgNP-assisted chemical etching, because a few Ag^+ ions may deviate from the as-deposited AgNPs and will be deposited on the side walls of the as-synthesized SiNWs. Fig. 6e–l suggest that increasing the etching temperature takes the similar effects as increasing the etching time. Note that the etching time should not be too long when the etching temperature is high, otherwise the well-aligned SiNWs would not be obtained for the drastic secondary AgNP-assisted chemical etching. We also carried out chemical etching of AgNP-coated Si wafers with high H_2O_2 concentration at room temperature. The surfaces of SiNWs are rough, similar to that of SiNWs produced with low H_2O_2 concentration at high temperature (∼60 °C) or for long etching time (60 min). However, the SiNWs are not well-aligned and with many fractures. We conclude that the smooth-surface SiNWs produced from Si(1 0 0, 1–10 Ω cm) wafers can only be obtained under the conditions of low H_2O_2 concentration (0.005–0.2 M) for short etching time (15–30 min) at low temperature (<25 °C), and the well-aligned SiNWs with rough surfaces can be prepared by appropriately increasing the etching time, etching temperature or H_2O_2 concentration.

To study the influence of the doping level of Si substrates on the surface topography of SiNWs, the heavily doped Si wafers with a resistivity of 0.005–0.025 Ω cm were used. The various morphologies of the SiNWs synthesized with different H_2O_2 concentrations are summarized in Fig. 7. The SiNWs prepared with 0.1 M H_2O_2 are rough and display low-density mesopores, as shown in Fig. 6c. With the increasing H_2O_2 concentration, both the surface roughness and

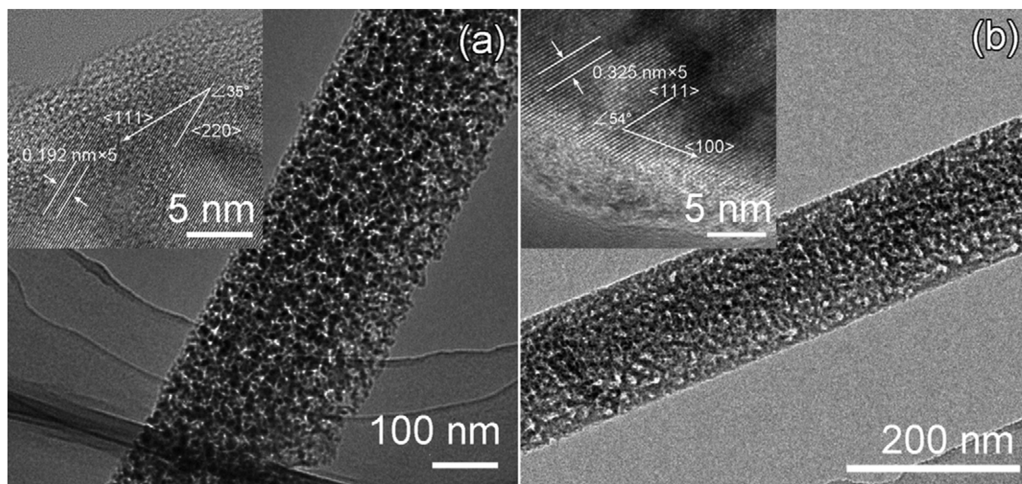

Fig. 5. TEM images of the individual SiNW from vertically- (a) and slantingly-aligned arrays (b). Insets are the corresponding HRTEM images.

the number of mesopores increase. In addition, the resulting SiNWs in the case show a significant increase in length, but a decrease in density. The similar trend is also observed for increasing the etching time. It can be understood as that the etching reaction is highly thermodynamically favored. Higher H_2O_2 concentration suggests an increase of the potential for the etching process [21]. Therefore, the driving force for the etching process is enhanced and thus increases the etching rate.

Fig. 6. SEM and TEM images of the SiNWs synthesized by chemical etching of Si(1 0 0, 1–10 Ω cm) wafers with AgNP deposition time of 1 min in 0.01 M $AgNO_3$/4.8 M HF and various etching conditions: in 0.2 M H_2O_2/4.8 M HF for 20 min at ∼20 °C (a–d); in 0.2 M H_2O_2/4.8 M HF for 60 min at ∼20 °C (e–h); in 0.2 M H_2O_2/4.8 M HF for 20 min at ∼60 °C (i–l); in 0.6 M H_2O_2/4.8 M HF for 20 min at ∼20 °C (m–p). (a, e, i and m) Cross-sectional views of the corresponding SiNWs. (b, f, j and n) Top views of the corresponding SiNWs. (c, g, k and o) Low-magnification TEM images of the corresponding SiNWs. (d, h, l and p) High-magnification TEM images of the corresponding SiNWs. Inset in (d) is HRTEM image of the corresponding SiNWs.

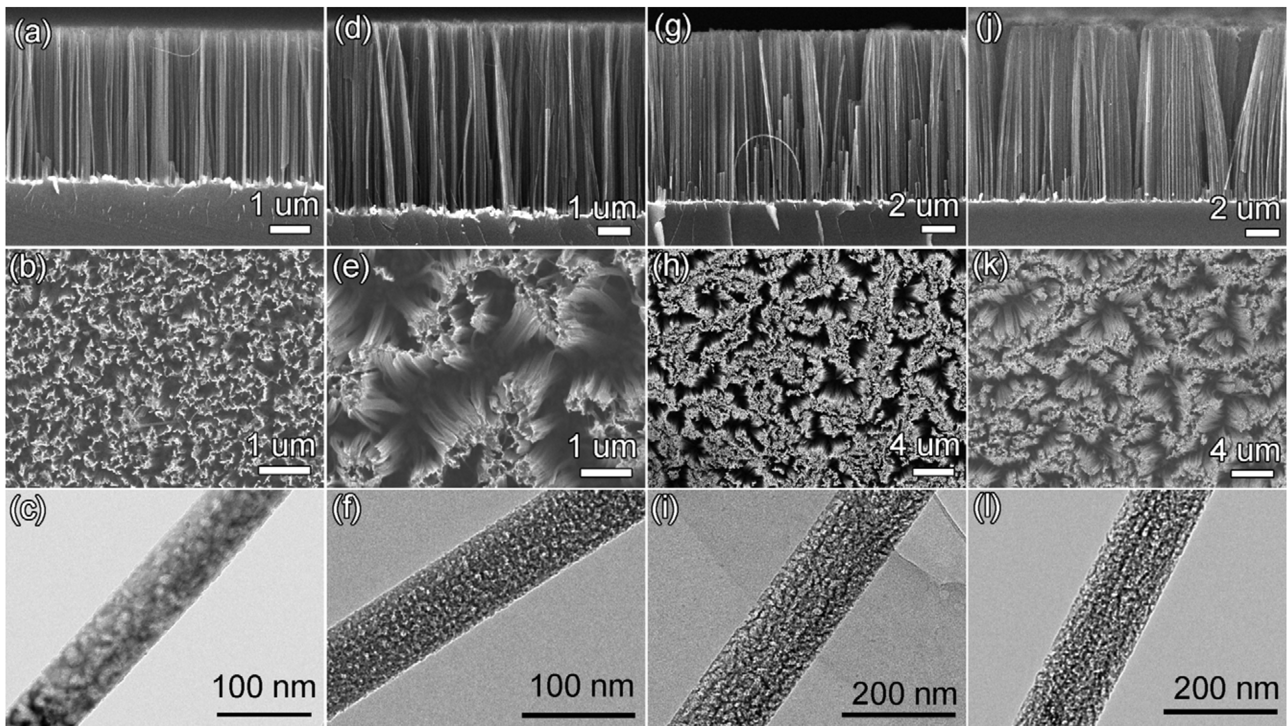

Fig. 7. SEM and TEM images of the SiNWs produced from Si(1 0 0, 0.005–0.025 Ω cm) wafers with AgNP deposition time of 1 min in 0.01 M $AgNO_3$/4.8 M HF and various etching solutions at room temperature for 30 min: 0.1 M H_2O_2/4.8 M HF (a–c); 0.2 M H_2O_2/4.8 M HF (d–f); 0.4 M H_2O_2/4.8 M HF (g–i); 0.8 M H_2O_2/4.8 M HF (j–l). (a, d, g and j) Cross-sectional views of the corresponding SiNWs. (b, e, h and k) Top views of the corresponding SiNWs. (c, f, i and l) TEM images of the corresponding individual SiNW.

The etching rate and surface topography of SiNWs also closely depend on the etching temperature. Fig. 8 shows the different morphologies of SiNWs prepared under the same conditions except for different temperatures. SEM images show that the SiNWs synthesized at 6 °C possess much higher density but smaller lengths relative to the ones synthesized at 60 °C. TEM images show that the surfaces of SiNWs prepared at high temperatures display uniform high-density mesopores, but the SiNWs prepared at low temperatures are with nonuniform sparse mesopores. Note that the crystal lattice is unbroken and continuous around the mesopores, suggesting that the mesoporous SiNWs is single crystalline.

Our results indicate that increasing the H_2O_2 concentration and etching temperature will result in an increase of surface roughness of SiNWs, and eventually mesoporosity. The appearance and increase of roughness and porosity of the SiNWs prepared from heavily doped Si wafers may be a result of one or two of the following factors. First, the SiNWs is formed by the chemical etching of Si at Ag/Si interfaces. However, the number of Ag^+ ions departing from the original AgNPs increases as the H_2O_2 concentration and etching temperature increase. Therefore, an increase of the amount of free Ag^+ will result in more and stronger secondary Ag-induced chemical etching on the side walls of the as-synthesized SiNWs, leaving higher roughness and mesopores on the surfaces

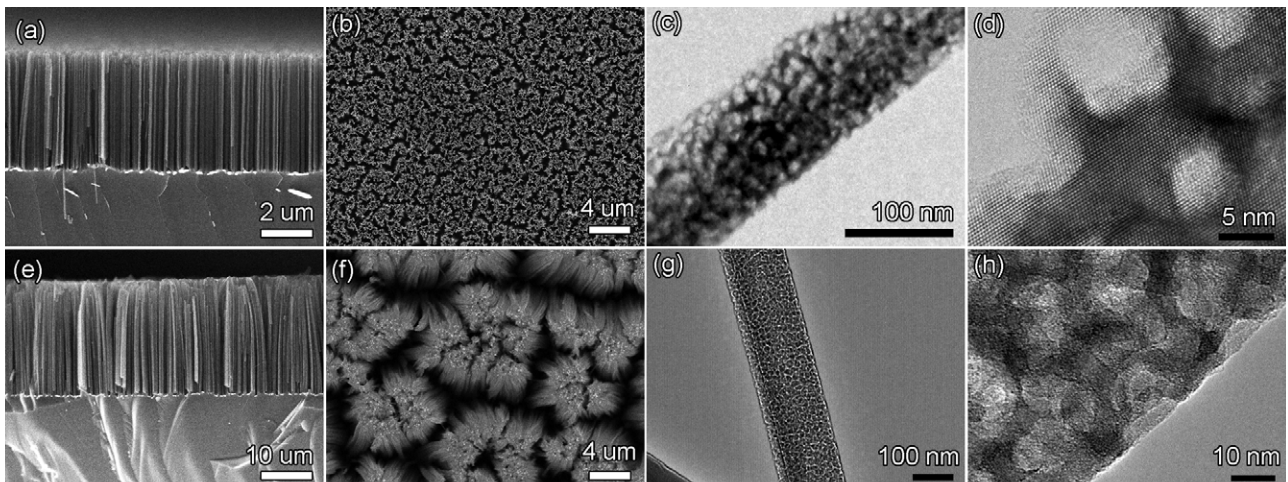

Fig. 8. SEM and TEM images of the SiNWs produced from Si(1 0 0, 0.005–0.025 Ω cm) wafers with AgNP deposition time of 1 min in 0.01 M $AgNO_3$/4.8 M HF and etched at various temperatures in 0.2 M H_2O_2/4.8 M HF for 20 min: ∼6 °C (a–d); ∼60 °C (e–h). (a and e) Cross-sectional SEM images of the corresponding SiNWs. (b and f) Top views of the corresponding SiNWs. (c and g) TEM images of the corresponding individual SiNW. (d) HRTEM image of the corresponding SiNW. (h) High-magnification TEM image of the corresponding SiNW.

of SiNWs. Second, since the crystal defects and impurities on the silicon surface are thought to serve as nucleation sites for pore formation in some models of porous silicon formation [22,23], a higher doping level may lead to a larger thermodynamic driving force for pore formation, thus increasing the etching rate and producing many mesopores. And another similar understanding is: a lower barrier will increase charge flow under the same potential, thus increasing the roughness and porosity in etching of porous silicon [24]. Hochbaum et al. proposed another factor of formation of mesoporous SiNWs: higher p-type dopant concentration lowers the energy barrier of charge injection across the Si surface, thus increasing current flow under the same applied bias [23]. According to their viewpoint, n-type wafers produced only rough nanowires without pores, regardless of the dopant concentration. However, our results of the mesoporous SiNWs prepared from n-type Si(1 1 1) wafers (as shown in Fig. 5) suggest that this viewpoint is not accounted for the formation of mesoporous SiNWs.

4. Conclusions

In summary, the well vertically- and slantingly-aligned SiNWs with ultra-high aspect ratio were prepared by chemical etching of Si(1 0 0) and Si(1 1 0) wafers, respectively. Zigzag SiNWs with various turning angles (90°, 125°, and 150°), as well as straight SiNWs, were obtained by chemical etching of Si(1 1 1) wafers by adjusting the AgNP moving direction in Si substrates, which is mainly determined by the orientation of Si substrates, size of AgNPs and chemical etching temperature. And the surface of SiNWs can be controlled to be smooth or rough, with or without mesopores. The effects of the etching conditions (etching time, etching temperature, H_2O_2 concentration and AgNP deposition time) and substrate properties (crystal orientation and doping level) on the morphology (vertically-aligned, slantingly-aligned, or curved; smooth or rough, with or without mesopores) of the resulting SiNWs are summarized in Table 1. According to Table 1 and our many other experiments, we conclude that:

(1) Etching time mainly affects the length and surface-roughness of the as-etched SiNWs. The SiNW length increases as the etching time increases, and the surface roughness will obviously increase when the etching time increases to long enough.
(2) AgNP-deposition time is closely related to the SiNW density and the AgNP-moving direction in Si(1 1 1) substrates. The AgNP density usually increases as the AgNP-deposition time increases, resulting in a decrease of the SiNW density. The AgNP size is also considered to increase as the AgNP-deposition time increases. The short AgNP-deposition time (small AgNP size) generally leads to the vertical etching of Si(1 1 1) substrates, the long AgNP-deposition time (large AgNP size) the slanting etching of Si(1 1 1) substrates. While the medial AgNP-deposition time usually induce a change of the AgNP moving directions in Si(1 1 1) substrates, leaving curved SiNWs with various turning angles.
(3) H_2O_2 concentration determines the rate of AgNP-induced Si etching. A higher H_2O_2 concentration means faster etching rate and more secondary etching. In other words, the length, density and surface-roughness of SiNWs increase with the increasing H_2O_2 concentration.
(4) Etching temperature influences the Si-etching rate and the AgNP-moving directions in Si(1 1 1) substrates. The higher the etching temperature, the faster the etching rate. And the AgNP-moving direction in Si(1 1 1) substrates can be changed from ⟨1 0 0⟩ to ⟨1 1 1⟩ directions when the temperature is improved from 20 °C to 50 °C.

Table 1
Summary of the effects of the etching conditions and substrate properties on the morphology of the resulting SiNWs.[a]

	Etching conditions								
	Etching time		AgNP-deposition time (in the solution of 0.005 M $AgNO_3$ and 4.8 M HF)			H_2O_2 concentration (mixed with 4.8M HF)		Etching temperature	
	Short (<30 min)	Long (>50 min)	Short (<60 s)	Medial (~120 s)	Long (>150 s)	Low (<0.2 M)	High (>0.4 M)	Low (<25 °C)	High (>50 °C)
Si(1 0 0) substrates low doping level (1–10 Ω cm)	Vertical, smooth	Vertical, rough, without mesopores	Vertical, smooth	Vertical, smooth	Vertical, smooth	Vertical, smooth	Vertical, rough, without mesopores	Vertical, smooth	Vertical, rough, without mesopores
Si(1 0 0) substrates high doping level (0.005–0.025 Ω cm)	Vertical, rough, With low-density mesopores	Vertical, rough, with high-density mesopores	Vertical, rough, with low-density mesopores	Vertical, rough, with low-density mesopores	Vertical, rough, with low-density mesopores	Vertical, rough, with low-density mesopores	Vertical, rough, with high-density mesopores	Vertical, rough, With low-density mesopores	Vertical, rough, with high-density mesopores
Si(1 1 0) substrates low doping level (75–150 Ω cm)	Slanting, smooth	Slanting, rough, without mesopores	Slanting, smooth	Slanting, smooth	Slanting, smooth	Slanting, smooth	Slanting, rough, without mesopores	Slanting, smooth	Slanting, rough, without mesopores
Si(1 1 1) substrates high doping level (0.01–0.02 Ω cm)	Slanting, rough, with low-density mesopores	Slanting, rough, with high-density mesopores	Vertical, rough, with low-density mesopores	Curved, rough, with low-density mesopores	Slanting, rough, with low-density mesopores	Slanting, rough, with low-density mesopores	Slanting, rough, with high-density mesopores	Slanting, rough, with low-density mesopores	Vertical, rough, with high-density mesopores

[a] *Note*: the variable of etching condition is single, besides the conditions marked as above, the other typical etching conditions are: 1 min of AgNP-deposition time in the solution of 0.01 M $AgNO_3$ and 4.8 M HF, 30 min of etching time in the solution of 0.2 M H_2O_2 and 4.8 M HF, room temperatures (~20 °C) of etching temperature. "*Vertical*" means the SiNWs are vertically-aligned relative to the substrate. "*Slanting*" means the SiNWs are slantingly-aligned relative to the substrate. "*Curved*" means the SiNWs are not straight (namely zigzag) and with a turning angle. "*Smooth*" or "*Rough*" mean the surfaces of SiNWs are smooth or rough. "*With or without mesopores*" means there are or not mesopores on the surfaces of SiNWs, and the "*low-density*" and "*high-density*" refer to the low- or high-density mesopores on the surface of SiNWs.

(5) Substrate properties have a direct relation to the SiNW orientation and their surface roughness. Si(1 0 0) substrates substantially lead to vertically-aligned SiNWs, Si(1 1 0) substrates slantingly-aligned SiNWs. While Si(1 1 1) substrates can induce to both the curved and straight SiNWs, which depends on the etching conditions. The doping level of substrates touches on surface roughness of the as-etched SiNWs—the higher the doping level, the larger the roughness. And the mesoporous SiNWs can be produced when the doping concentration is high enough (with a resistivity smaller than 0.01 Ωcm).

Furthermore, the facile morphological control of SiNWs supplies further understanding of the underlying metal-assisted chemical etching mechanisms, and the various morphologies of SiNWs make it possible to realize the wider or full potentials.

Acknowledgments

This work was supported by the National Basic Research Program of China (No. 2010CB832905), and partially by the Key Scientific and Technological Project of the Ministry of Education of China (No. 108124).

References

[1] D.K. Michael, W.B. Shannon, A.P. Jan, B.T.E. Daniel, C.P. Morgan, L.W. Emily, M.S. Joshua, M.B. Ryan, S.L. Nathan, A.A. Harry, Enhanced absorption and carrier collection in Si wire arrays for photovoltaic applications, Nature Materials 9 (2010) 239–244.
[2] A.K. Buin, A. Verma, A. Svizhenko, M.P. Anantram, Significant enhancement of hole mobility in [1 1 0] silicon nanowires compared to electrons and bulk silicon, Nano Letters 8 (2008) 760–765.
[3] G.J. Zhang, H.C. Jay, R.E. Chee, A. Agarwal, S.M. Wong, K.D. Buddharaju, N. Balasubramanian, Highly sensitive measurements of PNA-DNA hybridization using oxide-etched silicon nanowire biosensors, Biosensors and Bioelectronics 23 (2008) 1701–1707.
[4] J. Xiang, W. Lu, Y. Hu, Y. Wu, H. Yan, C.M. Lieber, Ge/Si nanowire heterostructures as high-performance field-effect transistors, Nature 441 (2006) 489–493.
[5] D.K. Michal, B.T.E. Daniel, M.K. Brendan, A.F. Michael, C.P. Morgan, S.L. Nathan, A.A. Harry, Photovoltaic measurements in single-nanowire silicon solar cells, Nano Letters 8 (2008) 710–714.
[6] H. Oliver, A. Ritesh, M.L. Charles, Nanoscale avalanche photodiodes for highly sensitive and spatially resolved photon detection, Nature Materials 5 (2006) 352–356.
[7] A.I. Hochbaum, R. Chen, R.D. Delgado, W. Liang, E.C. Garnett, M. Najarian, A. Majumdar, P. Yang, Enhanced thermoelectric performance of rough silicon nanowires, Nature 451 (2008) 163–168.
[8] Y.Y. Wu, P.D. Yang, Direct observation of vapor-liquid-solid nanowire growth, Journal of the American Chemical Society 123 (2001) 3165–3166.
[9] L.W. Yu, P.R.I. Cabarrocas, Growth mechanism and dynamics of in-plane solid–liquid–solid silicon nanowires, Physical Review B 81 (2010) 085323–085333.
[10] R.Q. Zhang, Y. Lifshitz, S.T. Lee, Oxide-assisted growth of semiconducting nanowires, Advanced Materials 15 (2003) 635–640.
[11] Y. Wang, V. Schmidt, S. Senz, U. Gösele, Epitaxial growth of silicon nanowires using an aluminium catalyst, Nature Nanotechnology 1 (2006) 186–189.
[12] J. Zhu, Z. Yu, G.F. Burkhard, C.M. Hsu, S.T. Connor, Y. Xu, Q. Wang, M. McGehee, S. Fan, Y. Cui, Optical absorption enhancement in amorphous silicon nanowire and nanocone arrays, Nano Letters 9 (2009) 279–282.
[13] Z.P. Huang, H. Fang, J. Zhu, Fabrication of silicon nanowire arrays with controlled diameter, length, and density, Advanced Materials 19 (2007) 744–748.
[14] K.Q. Peng, A.J. Lu, R.Q. Zhang, S.T. Lee, Motility of metal nanoparticles in silicon and induced anisotropic silicon etching, Advanced Functional Materials 18 (2008) 3026–3035.
[15] Z.P. Huang, N. Geyer, P. Werner, J. de Boor, U. Gösele, Metal-assisted chemical etching of silicon: a review, Advanced Materials 23 (2011) 285–308.
[16] F. Zhao, G.A. Cheng, R.T. Zheng, D.D. Zhao, S.L. Wu, J.H. Deng, Field emission enhancement of Au–Si nano-particle-decorated silicon nanowires, Nanoscale Research Letters 6 (2011) 176–180.
[17] R.L. Smith, S.D. Collins, Porous silicon formation mechanisms, Journal of Applied Physics 71 (1992) R1–R22.
[18] C.Y. Chen, C.S. Wu, C.J. Chou, T.J. Yen, Morphological control of single-crystalline silicon nanowire arrays near room temperature, Advanced Materials 20 (2008) 3811–3815.
[19] H. Fang, X.D. Li, S. Song, Y. Xu, J. Zhu, Fabrication of slantingly-aligned silicon nanowire arrays for solar cell applications, Nanotechnology 19 (2008) 255703–255708.
[20] H. Chen, H. Wang, X.H. Zhang, C.S. Lee, S.T. Lee, Wafer-scale synthesis of single-crystal ziazag silicon nanowire arrays with controlled turning angles, Nano Letters 10 (2010) 864–868.
[21] Y. Qu, L. Liao, Y. Li, H. Zhang, Y. Huang, X. Duan, Electrically conductive and optically active porous silicon nanowire, Nano Letters 9 (2009) 4539–4543.
[22] A.G. Cullis, L.T. Canham, P.D.J. Calcott, The structural and luminescence properties of porous silicon, Journal of Applied Physics 82 (1997) 909–965.
[23] A.I. Hochbaum, D. Gargas, Y.J. Hwang, P. Yang, Single crystalline mesoporous silicon nanowires, Nano Letters 9 (2009) 3550–3554.
[24] M.I.J. Beale, J.D. Benjamin, M.J. Uren, N.G. Chew, A.G. Cullis, An experimental and theoretical study of the formation and microstructure of porous silicon, Journal of Crystal Growth 73 (1985) 622–636.